Hindawi
Journal of Nanomaterials
Volume 2021, Article ID 8833864, 15 pages
https://doi.org/10.1155/2021/8833864

Research Article

Biosynthesis of Zinc Oxide Nanoparticles Using Aqueous *Piper betle* Leaf Extract and Its Application in Surgical Sutures

Quynh Mai Thi Tran,[1] Hong Anh Thi Nguyen,[2] Van-Dat Doan,[1] Quang-Hieu Tran,[3] and Van Cuong Nguyen[1]

[1]*Faculty of Chemical Engineering, Industrial University of Ho Chi Minh City, 12 Nguyen Van Bao, Go Vap, Ho Chi Minh City 70000, Vietnam*
[2]*Faculty of Chemical Engineering, Ho Chi Minh City University of Food Industry, 140 Le Trong Tan St, Ho Chi Minh City, Vietnam*
[3]*Department of Chemistry, Basic Sciences Department, Saigon Technology University, Ho Chi Minh City, Vietnam*

Correspondence should be addressed to Van Cuong Nguyen; nvc@iuh.edu.vn

Quynh Mai Thi Tran and Hong Anh Thi Nguyen contributed equally to this work.

Received 29 August 2020; Revised 3 January 2021; Accepted 13 January 2021; Published 13 February 2021

Academic Editor: Sheng-Joue Young

Copyright © 2021 Quynh Mai Thi Tran et al. This is an open access article distributed under the Creative Commons Attribution License, which permits unrestricted use, distribution, and reproduction in any medium, provided the original work is properly cited.

Surgical site infection (SSI), mainly caused by *Staphylococcus aureus* (*S. aureus*) and *Escherichia coli* (*E. coli*), is considered the most frequent complication in a surgical patient. Globally, surgical site infection accounts for 2.5%-41.9% and even higher rates in developing countries. SSI affects not only the patient's health but also the development of society. Like previous reports, a surgical suture increases the hazard of SSI due to its structure. The antibacterial suture is the most effective solution to decrease the SSI. Due to some unique properties, nano-zinc oxide (ZnO NPs) is one of the promising antibacterial agents for coating on the suture. In this study, we aim to synthesize the ZnO NPs using *Piper betle* leaf extract and used it to coat the suture. The effect of synthesis parameters on the size and morphology of ZnO NPs was studied as well. The UV-Vis spectrum indicated the formation of ZnO NPs with λ_{max} at around 370 nm. The volume of leaf extract plays a role in controlling the size and morphology of zinc oxide nanoparticles. The average particle size of as-synthesized ZnO NPs was around 112 nm with a hexagonal and spherical shape. Other than that, the results proved that ZnO NPs performed a high antibacterial activity against S. aureus and E. coli with its antibacterial effectiveness up to 5 days. The ZnO NP-coated sutures also exhibited a high performance on bacterial inactivation. With key findings, this study made a tremendous contribution to lowering the burden on medical services in terms of medical treatment cost in developing countries.

1. Introduction

Surgical site infections (SSIs) are one of the most common healthcare-associated infections (HAI) in developing countries, with up to 30 days of infection after surgery (or up to one year in patients receiving implants) [1–5]. SSIs are usually caused by *Staphylococcus aureus* (*S. aureus*) and *Escherichia coli* (*E. coli*) [3, 4]. These bacteria can be found from a patient's own body (endogenous infection) or from the external environment (exogenous infection) during the surgery or after that. Almost all SSIs are due to the invasion of bacteria during surgery, leading to more serious consequences within 5-7 days after surgery.

Although hospitals have been implementing preventions strictly, there is no significant effect. It is reported that the invasion of external bacteria from surgical sutures, especially braided multifilament sutures, is one of the factors to increase rates of surgical infection [6–10]. Braided multifilament sutures provide a larger surface area than monofilament sutures, resulting in greater bacterial adherence.

To reduce bacterial colonization, scientists and manufacturers have introduced a coating that contains antiseptic

agents such as triclosan (TC), chlorhexidine, polyhexamethylene biguanide (PHMB), and octenidine. The TC-coated surgical suture has been approved by the Food and Drug Administration (FDA) as an effective antibacterial surgical suture [8–11] and commercialised since 2002. However, there are arguments about the impact of TC on human health. Triclosan affects immune responses, ROS production, and cardiovascular functions which were reported somewhere [12].

The development of nanotechnology has distributed astonishing progress in industry, computing, medicine, etc., and even in the health care system. Silver nanoparticles (Ag NPs) have been widely used as an effective antimicrobial agent coating on wound dressing, catheter, etc. [13]. Nevertheless, there is no regulation which is clear enough for risk management of silver nanoparticles in implant medical devices. On the other hand, the human body is not able to discrete silver or silver ions, resulting in an accumulation of silver as well as destruction of DNA and red blood cells [14–16].

Unlike other metals or metal oxides, zinc oxide (ZnO) or zinc oxide nanoparticle (ZnO NP) is approved by FDA due to its biodegradability, low toxicity, and economy so it has been used in an increasing number of industrial products such as paint, coating, cosmetic, and biomedicine in the past two decades, especially in the discipline of anticancer or antibacterial fields [17, 18]. Nowadays, increasing studies demonstrate the good antibacterial properties and biocompatibility of ZnO NPs [19–27]. Because of the limitation of chemical reagents as well as their residue after reaction, physical and chemical methods are not the priority for ZnO NP preparation in the medical field. The development of green chemistry has attracted increasing attention since it is believed to be nontoxic, eco-friendly, and biocompatible. Recently, many reviews on green technology-based synthesis of nanoparticles have shown that they are promising methods for large-scale production of metal nanoparticles for biomedical applications. A wide variety of plant extracts are used for the biosynthesis of ZnO NPs, and the results proved that ZnO NPs are safe for human use alternative to Ag NPs or other metal nanoparticles [28–34]. *Piper betle L*. known as a traditional herbal medicinal plant is associated with the control of caries and periodontal disease, inflammation, antimicrobial activity, etc. [35–42]. Recently, *Piper betle L*. has been used as a reductant and capping agent in metal nanoparticles such as Ag NPs, gold nanoparticles (Au NPs), and copper oxide nanoparticles (CuO NPs) [43–45] owing to organic compounds in *Piper betle* extract (hereinafter called as ET) [35]. Until now, there are only a few studies using *Piper betle L.* extract to fabricate the ZnO NPs and evaluate its biocompatibility *in vitro* such as those by Song and Yang and Shubha et al. [28, 46]. From the aspect of medical implants, we aim to synthesize ZnO NPs using *Piper betle* leaf extract and investigate the effect of parameters on the ZnO NP formation. Then, the antibacterial activity of as-prepared ZnO NPs was investigated against *E. coli* and *S. aureus*. Finally, ZnO NPs were coated on the braided multifilament surgical suture.

As mentioned above, Song and Yang [28] evaluated the cytotoxicity towards human osteoarthritic chondrocytes of ZnO NPs using *Piper betle* leaf extract. Zinc nitrate ($ZnNO_3$) and aqueous *Piper betle* leaf extract were used as precursors. In this study, water was used as a solvent during extraction instead of other solvents. It was explained that water is favourable for extracting polyphenols contained in *Piper betle* leaves. Besides, water is known as a green solvent, so it is safe for human use. The result showed that the plant extract is of negligible cytotoxicity, indicating that the cytotoxicity is due to the ZnO NPs. The NPs exhibited concentration-dependent cytotoxicity, but even at high concentrations (80-100 ppm), biocompatibility of ZnO NPs was still proved. In 2018, Shubha and his colleagues [46] also studied ZnO NPS synthesized by using aqueous *Piper betle* leaf extract against dental pathogens. As a result, ZnO NPs with smaller size (~69 nm) exhibited more potent antibacterial activity to bacteria, namely, *Streptococcus mutans* (*S. mutans*) and *Lactobacillus acidophilus* (*L. acidophilus*).

Based on these references, water and $ZnNO_3$ were chosen as extracting solvents and precursors, respectively. Although previous studies showed good to excellent antimicrobial activity, the effectiveness of ZnO NPs which plays an important role in the prevention of surgical site infection was still unknown. Therefore, this property is investigated in this study as well.

2. Materials and Methods

2.1. Materials. Zinc nitrate hexahydrate (CAS 10196-18-6, AR Grade) and ethanol absolute (CAS 64-17-5, AR Grade) were purchased from TCI, Japan. *Piper betle* leaves were purchased from the local market and cleaned with deionized water, followed by drying under sunlight. The dry leaves were then crushed into powder and stored in air-tight containers.

2.2. Preparation of Piper betle Leaf Extract (ET). This study is aimed at finding out the optimum parameters for the extraction of components from *Piper betle* leaf using deionized water (18.2 mΩ·cm resistivity) [28, 42, 46–48]. The optimum conditions were selected based on the extract yield by varying parameters: (1) ratio between material amount (g) and solvent volume (ml) (1 : 5, 1 : 10, and 1 : 15, *w*/*v*), (2) extraction temperature (70, 80, and 90°C), and (3) extraction time (15, 30, and 60 minutes). Briefly, a given amount of powder (2, 1, and 0.67 g) was mixed with deionized water to obtain the ratio 1 : 5, 1 : 10, and 1 : 15 (*w*/*v*). The mixture was then boiled for a specific time (15, 30, and 60 minutes) at different temperatures (70, 80, and 90°C). After cooling, the solution was filtered through a 0.45 μm filter membrane (Whatman filter paper). The extract was freeze-dried for 48 h to obtain the solid extract. The extract was weighed and recorded. The dried and solution extract was stored in a refrigerator for further use.

2.3. Biosynthesis of Zinc Oxide Nanoparticles. In brief, a measured volume of leaf extract was dropped-wise into 100 ml of zinc nitrate solution at different concentrations under ultrasonic bath, obtaining the ratio between volume of extract and Zn^{2+} solution as 1 : 1, 1 : 5, and 1 : 10. The aqueous reaction solution was then sonicated until a pale yellow

precipitate was observed. The precipitate was centrifuged and washed several times with double distilled water and absolute ethanol before drying and annealing at 600°C to obtain a white powder of ZnO NPs.

According to previous reports, the concentration of zinc salt, volume of extract, and pH affect the formation of ZnO NPs [30, 49–51]. It was noted that the ZnO NPs were formed only at pH 5-7 or pH 8 [49, 52]. While a total reduction of zinc nitrate to zinc oxide nanoparticles occurred at pH 8, an aggregation of zinc oxide nanoparticles to form larger nanoparticles was proceeded at pH 5-7. The pH of the extract is usually about 6–6.5, so it is necessary to use more chemical reagents to reach pH 8, leading to probable cytotoxicity as mentioned in Shubha et al.'s study [46]. Therefore, pH 5-7 was chosen in this study.

Nagarajan and Kuppusamy [52] concluded that the formation of ZnO NPs starts since the concentration of zinc ion (Zn^{2+}) is 1 mM. When the concentration of Zn^{2+} goes up to 0.01 M, a pale precipitate appears. This could be explained due to more nanoparticles formed, leading to the aggregation of the larger size of nanoparticles [53, 54]. Hence, the concentration of Zn^{2+} in this study was 0.001, 0.01, and 0.1 M, respectively.

The particle size of ZnO NPs depends on the volume of plant extract [50, 51]; the more volume of plant extract, the smaller the size of ZnO NPs. The size dependence was evaluated through the ratio between volume of extract and volume of Zn^{2+}. The ratios 1 : 1, 1 : 5, and 1 : 10 were selected in this study.

2.4. Characterization. The optical absorbance of samples was analysed using a UV-Vis spectrophotometer (UV-1900, Shimadzu, Japan). Morphology of ZnO NPs was determined using a Scanning Electron Microscope (SEM) at Saigon Hi-tech Park Laboratory (SHTP Lab), Ho Chi Minh, Viet Nam (HiTachi S-4800, Tokyo, Japan). The crystal structures of ZnO NPs were analysed using XRD (LabX XRD-6100, Shimadzu, Japan) from 10° to 80° in 2θ steps using Cu K_α radiation. FT-IR spectroscopy instrument (Tensor 27, Bruker, Germany, 4000-400 cm^{-1}) was used to measure the surface capping groups on NPs. A small amount of sample was mixed with KBr and finely ground; then, this mixture was pressed to get a homogeneous and transparent film. The size distribution of ZnO NPs was determined using a DLS instrument (SZ 100, Horiba, Japan).

2.5. Bacteriological Studies. The antibacterial activity and its effectiveness were determined using the agar disk diffusion method [46, 55]. In order to identify how the extract influences the antibacterial ability of the material, both extract and ZnO NPs were used. Agar plates were inoculated with bacteria (*E. coli* ATCC 25922 or *S. aureus* ATCC 25923) or control (gentamicin antibiotic 10 μg). Then, filter paper disks (about 6 mm in diameter), containing ZnO NP solution or extract, were placed on the agar surface. The Petri dishes were then incubated at 37°C for 24 h and observed for growth or inhibition. The sample positions are illustrated in Figure 1.

After investigating the bactericidal ability, the antibacterial effectiveness was conducted. The agar diffusion method was also used. The results were recorded after 48 (2 days), 72 (3 days), and 120 (5 days) hours of incubation. Figure 2 exhibits the sample position on the disk.

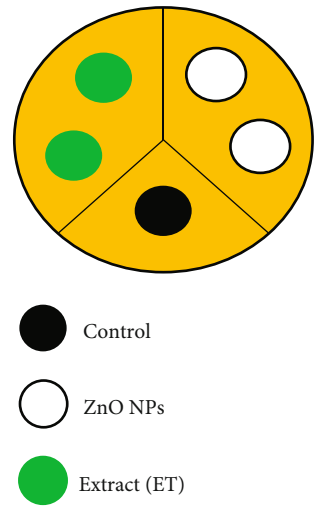

Figure 1: Illustration of sample position on the agar disk in bactericidal ability test.

For the coated surgical suture, the AATTC Test Method 147-2004 Parallel Streak Method was applied. Specimens of the test suture (about 5 cm in length) including the corresponding untreated suture of the same material (control) were placed in intimate contact with the agar surface which has been previously streaked with inoculums of bacteria (*E. coli* ATCC 25922 or *S. aureus* ATCC 25923) (Figure 3). After incubation at 37°C for 24 h, the zone of inhibition (ZOI) was observed.

The ZOI is calculated using the following equation:

$$W = \frac{(T - D)}{2}, \quad (1)$$

in which W is the width of ZOI (mm), T is the total diameter of the test specimen and ZOI (mm), and D is the diameter of the test specimen (mm).

2.6. Statistical Analysis. Experiments were performed in triplet for each parameter. Differences between the mean values were analysed using one-way analysis of variance (ANOVA) with $p < 0.05$.

3. Results and Discussion

3.1. Preparation of Piper betle Leaf Extract. As reported, the extraction yield was affected by various parameters such as the ratio of solid to liquid (w/v), extraction time, and extracted temperatures. In 2015, Foo and his colleagues [48] revealed that the yield of extraction of aqueous-based solvent *Piper betle* extract was higher than that of ethanol-based solvent extract. Therefore, water was used as a solvent in this study.

As shown in Figure 4, the color of the filtrated solution was transparent yellow and changed to brown powder after solvent evaporation. Figure 5 exhibits the optical absorption

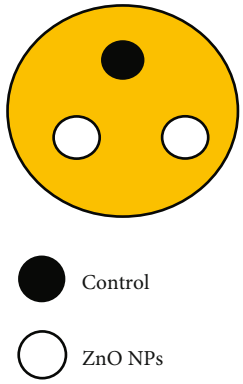

Figure 2: Illustration of sample position on the agar disk in antibacterial effectiveness test.

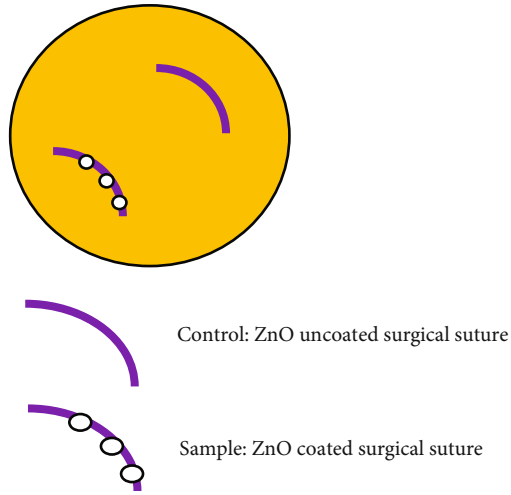

Figure 3: Illustration of sample position of surgical sutures on the agar disk in antibacterial test.

peak of ET at 280 and 325 nm as a previous report [28]. After freeze-drying, a brown powder was observed (Figure 4(c)), and the mass extraction and corresponding yield (%) are assumed in Table 1.

3.2. Effect of Parameters on the Extraction Yield. Various parameters ((1) ratio of solid-liquid (1 : 5, 1 : 10, and 1 : 15) (*w*/*v*), (2) extraction temperature (70-90°C), and (3) extraction time (15-60 minutes)) were investigated to obtain the maximum percentage of the extract (ET).

3.2.1. Effect of Ratio of Solid-Liquid and Time. To evaluate the effect of the ratio of solid-liquid on extraction yield, the temperature was kept constant at 90°C due to the higher solubility of polyphenols in water for a short time [28].

As seen in Figure 6, the yield of extraction increased when the ratio of solid-liquid decreased and reached to maximum after 30-minute extraction. Then, the yield started decreasing. It could be due to the competition of interaction between the solvents and material and/or because of the solvent evaporation during extraction.

It was noted that when the material mass was 2 grams per 10 ml (equilibrating to a ratio of 1 : 5), it was difficult for the solvent to assess the material which resulted in the low efficiency of extraction.

Last but not least, when the ratio of solid to liquid was 1 : 10 (1 gram per 10 ml), the yield was likely unchanged after 30-minute extraction which was chosen for further experiments.

3.2.2. Effect of Temperature. To investigate the effect of temperature on the yield extraction, the ratio 1 : 10 and time of 30 minutes were kept constant. The results from Table 2 and Figure 7 exhibited that the extraction yield increases with the increase of temperature. In a short period, the yield of extraction mainly depended on the temperature. It has been observed that the higher the temperature, the higher the yield of extraction. It could be because the temperature promotes the solubility of organic compounds in water [28].

From the point of view of the production scale, the optimal extraction conditions corresponded to the ratio between solid and liquid, temperature, and time which are 1 : 10, 90°C, and 30 min, respectively.

3.3. Biosynthesis of Zinc Oxide Nanoparticles. The formation of ZnO NPs was confirmed by the appearance of precipitate (Figure 8(a)). This precipitate was in brown powder after freeze-drying (Figure 10(a)) due to the coverage of phytochemicals in the extract, which evaporated under high-temperature calcination leaving the white powder (Figure 8(c)). The UV-Vis spectrum showed sharp absorption peaks at 358, 368, and 378 nm (Figure 9), indicating the presence of as-prepared ZnO NPs. This result was in agreement with other references [46].

3.3.1. Effect of Zinc Salt Concentration on the Formation of ZnO NPs. Various parameters were selected to investigate their effect on ZnO NP formation. The experimental parameters are summarized in Table 3. The results in Figure 10 confirmed the statement that ZnO NPs started to form since the concentration of Zn^{2+} is 0.001 M, and the precipitate was observed when the concentration of Zn^{2+} was equal to or larger than 0.01 M.

Particle size measurement was conducted by using the DLS technique. Table 3 summarizes the average particle size of as-prepared ZnO NPs. When the concentration of zinc salt was less than 0.1 M, zinc ions acted as a controller of nucleation; the particles distributed from 100 to 200 nm with average size (*Z*-average) of 112.9 nm. Besides, its polydispersity index (PDI) was in the average range ($0.3 < \text{PDI} < 0.5$) (Figure 11). Once the concentration reached 0.1 M, PDI increased (PDI > 1), resulting in the aggregation of smaller particles to form bigger particles. For this reason, the DLS technique was not appropriate.

It has been established earlier that larger size nanoparticles of ZnO showed comparatively lower toxicity [46]. Other than that, the storage of the solid state was more favourable in comparison with the liquid state. Therefore, the concentration of 0.1 M of Zn^{2+} was selected for further experiments.

3.3.2. Effect of Liquid to Liquid Ratio on the Size and Morphology of ZnO NPs. To understand how the extract

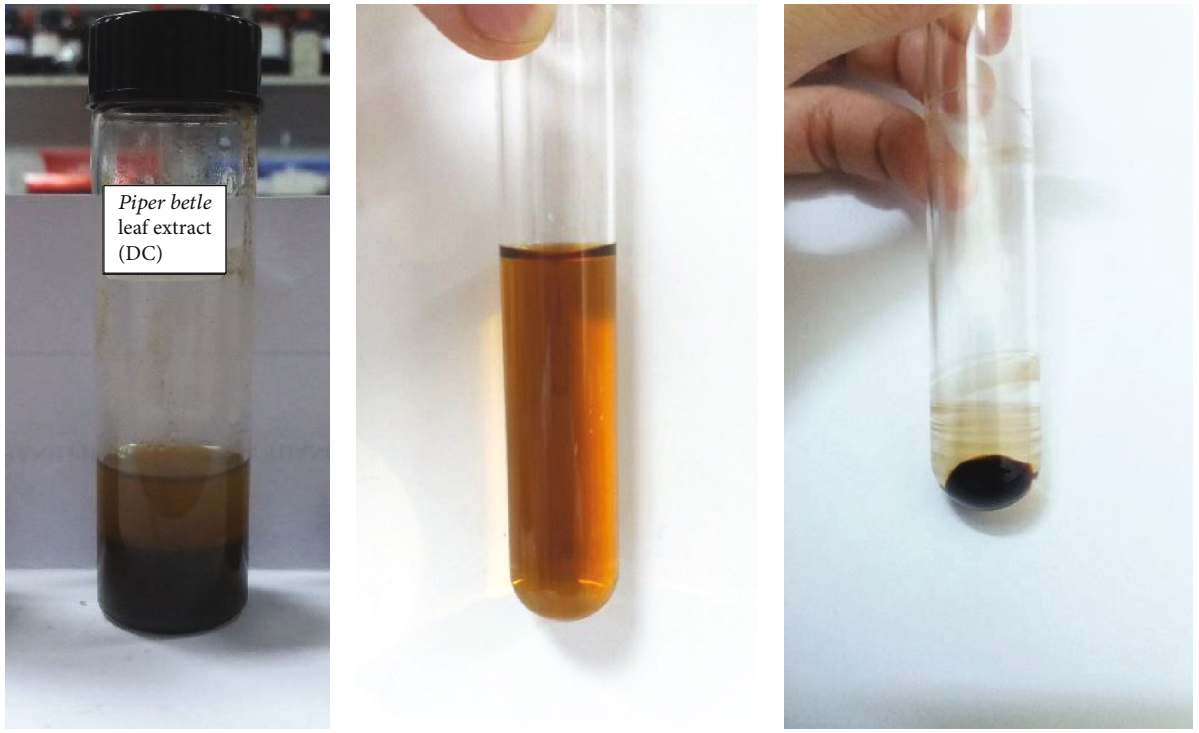

Figure 4: The color change of *Piper betle* extract: (a) color of extract before filtration, (b) color of extract after filtration, and (c) color of dried extract.

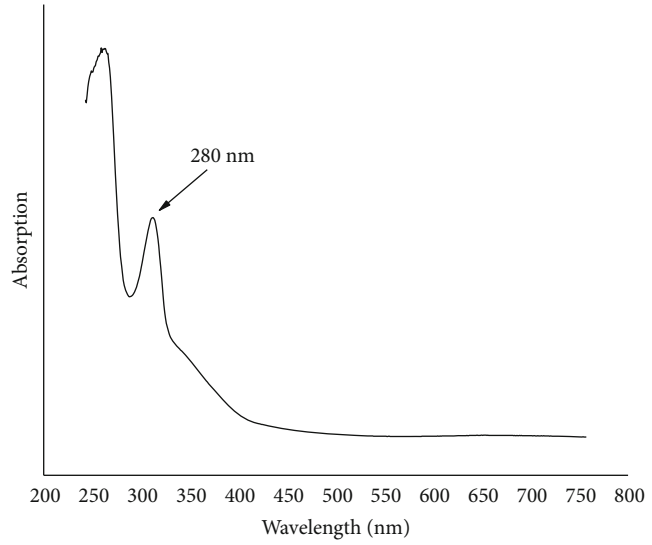

Figure 5: UV-Vis spectrum of *Piper betle* leaf extract.

volume affects the size and the morphology of ZnO NPs, 10, 20, and 100 ml of extract were added to 100 ml of aqueous Zn^{2+} solution under ultrasonic bath for 4 hours. The weights of dried ZnO NPs and sintered ZnO NPs are summarized in Table 4. It was clear that the product weight increases when the volume of extract increases. Hence, the ratio 1 : 1 was chosen to maximize the product quantity.

As shown in SEM results, the volume of extract played a role in controlling the size and morphology of ZnO NPs (Figure 12). When the volume of ET increased from 10 to 100 ml, the size of particles reduced and specific morphology was formed [50, 51]. Besides, the aggregation due to the pH at 5-7 was clearly observed. Figure 13 exhibits the morphology of ZnO NPs sintered at a higher temperature (600°C).

Table 1: Experimental results for preparation of *Piper betle* leaf extract using water solvent.

No.	Code	Material quantity (g)	Extraction time (min)	Mass of extract (g)	Yield (%)
1	ET1	2	15	0.23	11.5
2	ET2	2	30	0.3	15
3	ET3	2	60	0.13	6.5
4	ET4	1	15	0.21	21
5	ET5	1	30	0.24	24
6	ET6	1	60	0.23	23
7	ET7	0.67	15	0.15	22.4
8	ET8	0.67	30	0.2	29.9
9	ET9	0.67	60	0.17	25.4

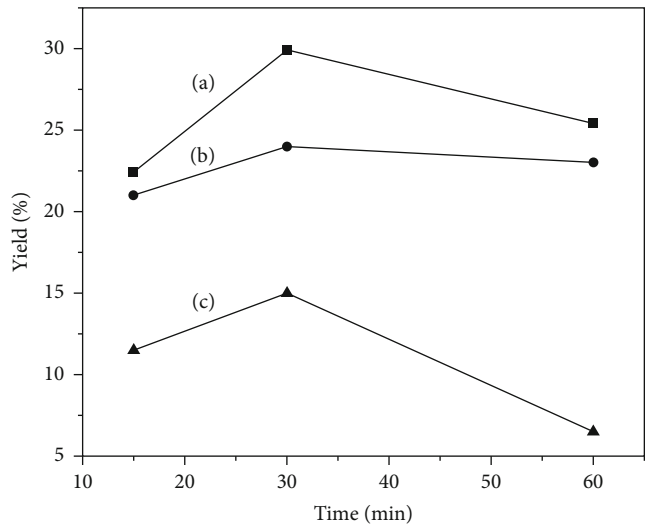

Figure 6: Effect of material quantity on extraction yield (a) ratio of 1 : 15, (b) ratio of 1 : 10, and (c) ratio of 1 : 5.

Table 2: Effectiveness of temperature on yield extract.

No.	Code	Extraction temperature (°C)	Mass of extract (g)	Yield (%)
1	ET10	70	0.12	12
2	ET11	80	0.21	21
3	ET12	90	0.24	24

ZnO NPs had a nearly hexagonal shape and spherical shape which could be explained by the functional group of compounds in the extract [30, 49].

FT-IR analysis was used to measure the functional groups in ET and ZnO NPs. Figure 14(a) confirms the presence of organic compounds such as amines, carboxylic acids, alkanes, esters, and alkenes with the absorption peaks at 3477.51, 2888.25, and 1637.27 cm^{-1}, ranging from 1416.62 to 956.62 cm^{-1}. In the spectrum of ZnO NPs (Figure 14(b)), the absence of peaks from 1416.62 to 956.62 cm^{-1} demonstrated the removal of almost all organic compounds after sintering. It is noted that the presence of a peak at 463.92 cm^{-1} contributed to the formation of ZnO NPs which complies with the color change of product after calcination (Figure 8).

Diffraction peaks of ZnO NPs were observed at 2θ values of 33.6°, 34.5°, 35.2°, 56.8°, 62.6°, 69.5°, and 70.2° corresponding to lattice planes (100), (002), (101), (103), (200), (112), and (201), respectively (Figure 15). The peaks are attributed to the hexagonal phase of ZnO (JCPDS 36-1451). There were still some impurity peaks due to the plant extract residues. Crystallite size (D) of NPs calculated by Scherrer's equation was 6.87 nm.

3.4. Bacteriological Studies

3.4.1. Role of ET and ZnO NPs in the Bacterial Ability. The antibacterial activity of ZnO NPs and its effectiveness was assayed against two major bacteria *E. coli* and *S. aureus*, respectively, by the agar disk diffusion method. The minimum inhibitory concentration for zinc oxide nanoparticles was 0.41 mg/ml for *E. coli* and 0.81 mg/ml for *S. aureus*, respectively. The minimum bactericidal concentration was 0.81 mg/ml for E. *coli* and 1.62 mg/ml for *S. aureus*, respectively. The ZOI of ZnO NPs was determined and calculated from equation (1) with the diameter of filter paper being

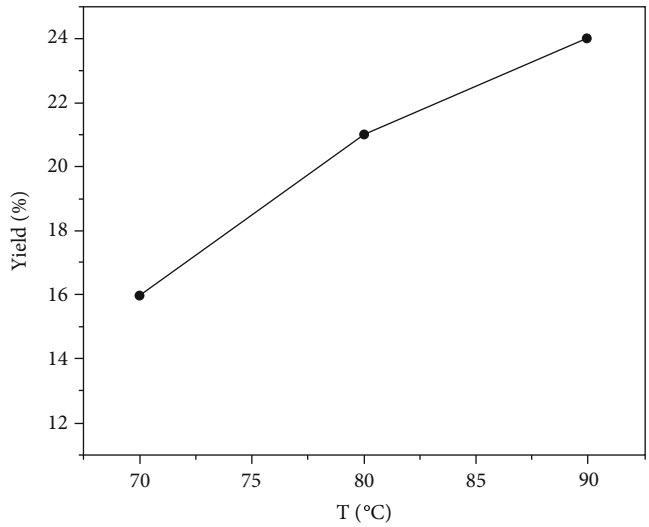

Figure 7: Effect of temperature on extraction yield.

(a) (b) (c)

Figure 8: (a) The presence of as-synthesized ZnO NPs; (b) color of ZnO NPs before calcination; (c) color of ZnO NPs before calcination.

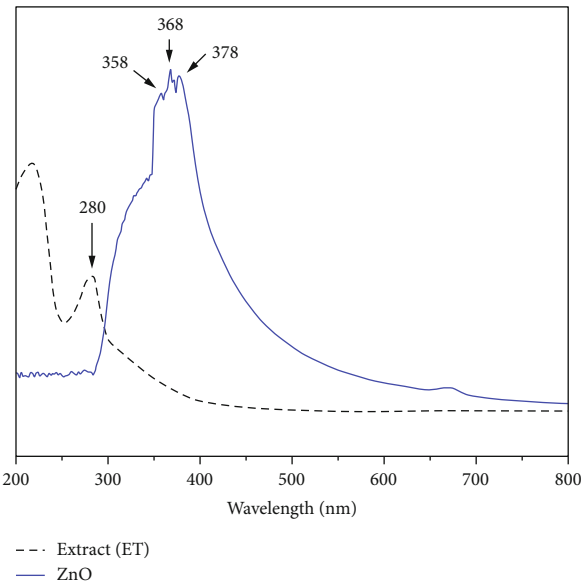

Figure 9: UV-Vis spectra of ET and ZnO NPs.

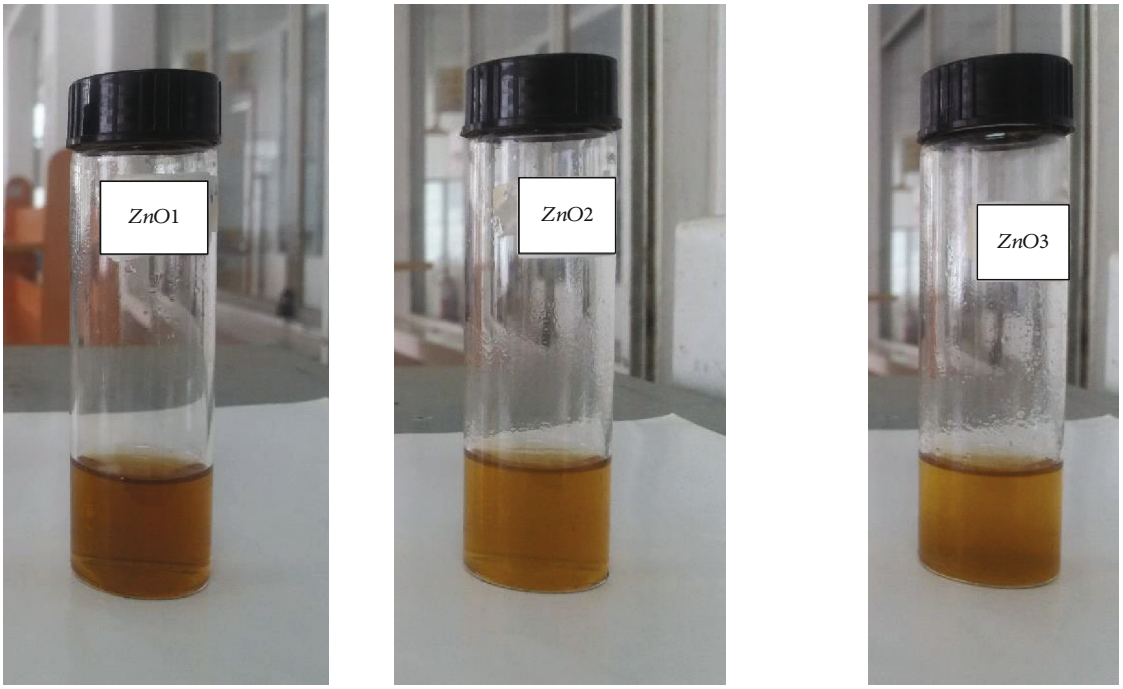

(a) ZnO NPs 1: transparent solution (b) ZnO NPs 2: precipitate starts to be observed (c) ZnO NPs 3: precipitate was observed clearly

Figure 10: Effectiveness of zinc ion concentration on ZnO NP formation.

Table 3: Experimental parameters used in ZnO NP synthesis.

No.	Code	$[Zn^{2+}]$ (M)	$\frac{V_{ET}}{V_{Zn^{2+}}}$	Reaction time (h)	(Z-average) (nm)	PDI
1	ZnO NPs 1	0.001	1 : 1	4	112.9	0.330
2	ZnO NPs 2	0.01	1 : 1	4	3640.2	1.018
3	ZnO NPs 3	0.1	1 : 1	4	3791.8	5.161

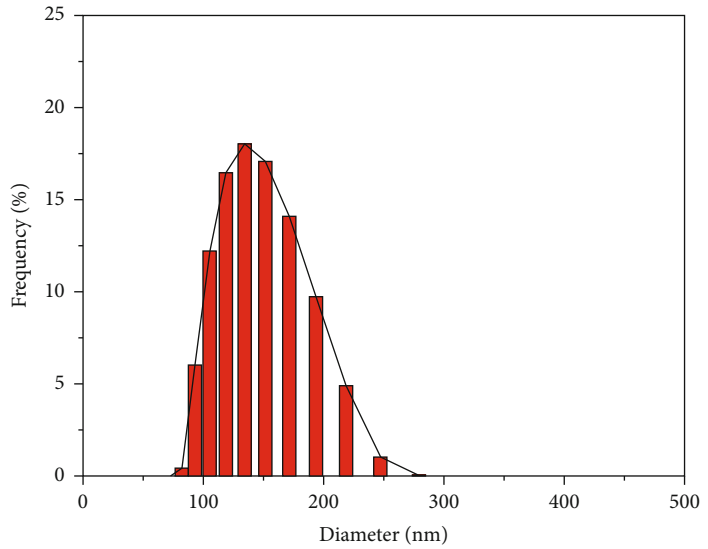

Figure 11: Dynamic light scattering (DLS) of ZnO NPs at a concentration of 0.001 M.

Table 4: The experiment results of ZnO NP synthesis using various volumes of ET and time.

No.	Code	$[Zn^{2+}]$ (M)	V_{ET} (ml)	$\frac{V_{ET}}{V_{Zn^{2+}}}$	Reaction time (h)	Mass of dried ZnO NPs (g)	Mass of sintered ZnO NPs (g)
1	ZnO NPs 4	0.1	10	1 : 10	4	0.005	0.003
2	ZnO NPs 5	0.1	20	1 : 5	4	0.030	0.010
3	ZnO NPs 6	0.1	100	1 : 1	4	1.158	0.080

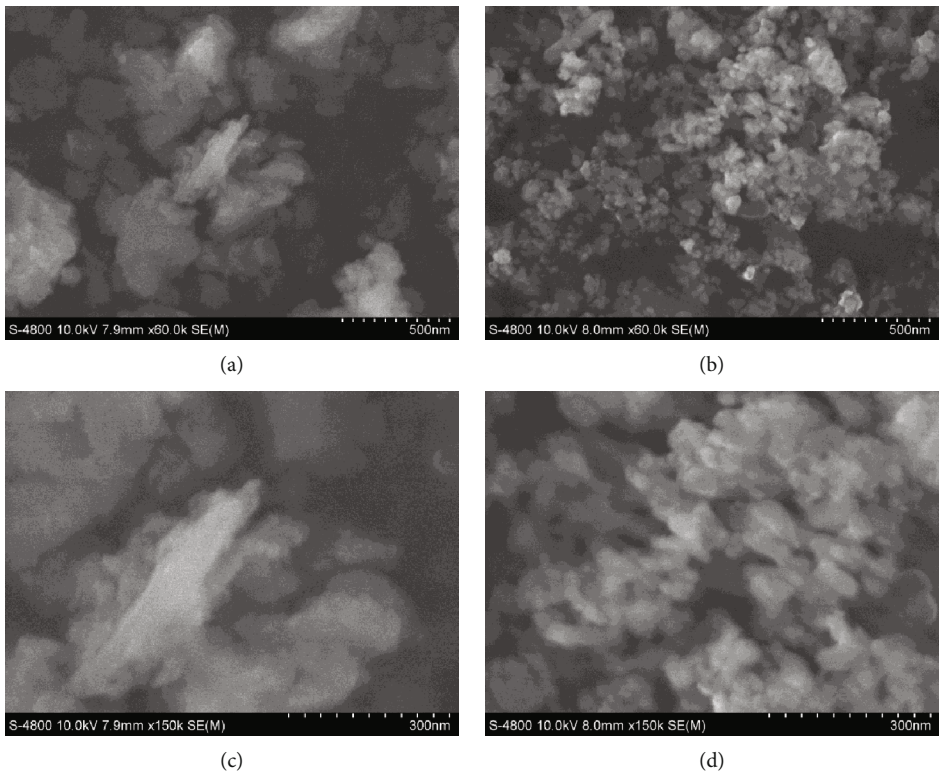

Figure 12: SEM images of synthesized ZnO NPs using different volumes of ET. SEM images of ZNO NPs using 10 ml of ET at magnification of (a) 60k and (c) 150k. SEM images of ZNO NPs using 100 ml of ET at magnification of (b) 60k and (d) 150k.

6 mm and that of suture (USP 1) being 0.4 mm. As seen in Figure 16, the bactericidal properties were due to ZnO NPs. The extract only played a role as reductants and capping agents and morphology controller.

As a result in Table 5, the ZOI of ZnO NPs on *E. coli* after 24 h incubation were quite small; it could be because of differences in the structure of bacteria [50]. In this study, the particle size of ZnO was bigger than 10 nm so the particles had adhered to the outer layer of bacteria plasma membranes, increased the surface tension, and inhibited the polarization of the membrane, allowing ZnO NP molecules to internalize into the cell. However, the cell membrane of *E. coli* has an additional outer plasma membrane, leading to slower diffusion of nanoparticles into the cell structure compared with the *S. aureus*. Therefore, the number of ZnO NPs that entered *E. coli* was less than that of *S. aureus* in 24 h.

3.4.2. Antibacterial Effectiveness of ZnO NPs. As seen in Figure 17, the bactericidal effectiveness of ZnO NPs could reach five days on both *E. coli* and *S. aureus*. The ZOI of nanoparticles increased after 48 h of incubation and maintained until five days (Table 5). This result met our requirement expectation that ZnO NPs could reduce the SSI within 5-7 days after surgery. It was noted that the ZOI of ZnO NPs after 48, 72, and 120 h of incubation on *E. coli* was better than that of the first 24 h. It might be explained as follows.

As the peptidoglycan of *E. coli* is thinner compared with that of *S. aureus*, ZnO NPs passed through the outer membrane of the bacteria cell easier. Here, the nanoparticles generate free electrons, which react with oxygen inside the bacteria cell. As a result, reagent oxygen species (ROS) are formed according to equations (2)–(4). These ROS will destroy protein structures and DNA structure leading to cell death. ROS was considered the antibacterial mechanism in this study:

$$O_2 + e^- \longrightarrow O_2 \quad (2)$$

$$O_2 + H_2O \longrightarrow HO_2 + HO^- \quad (3)$$

$$HO_2 + HO_2^{\cdot} \longrightarrow H_2O_2 + O_2 \quad (4)$$

$$H_2O_2 + O_2^{\cdot} \longrightarrow HO^{\cdot} + HO^- + O_2 \quad (5)$$

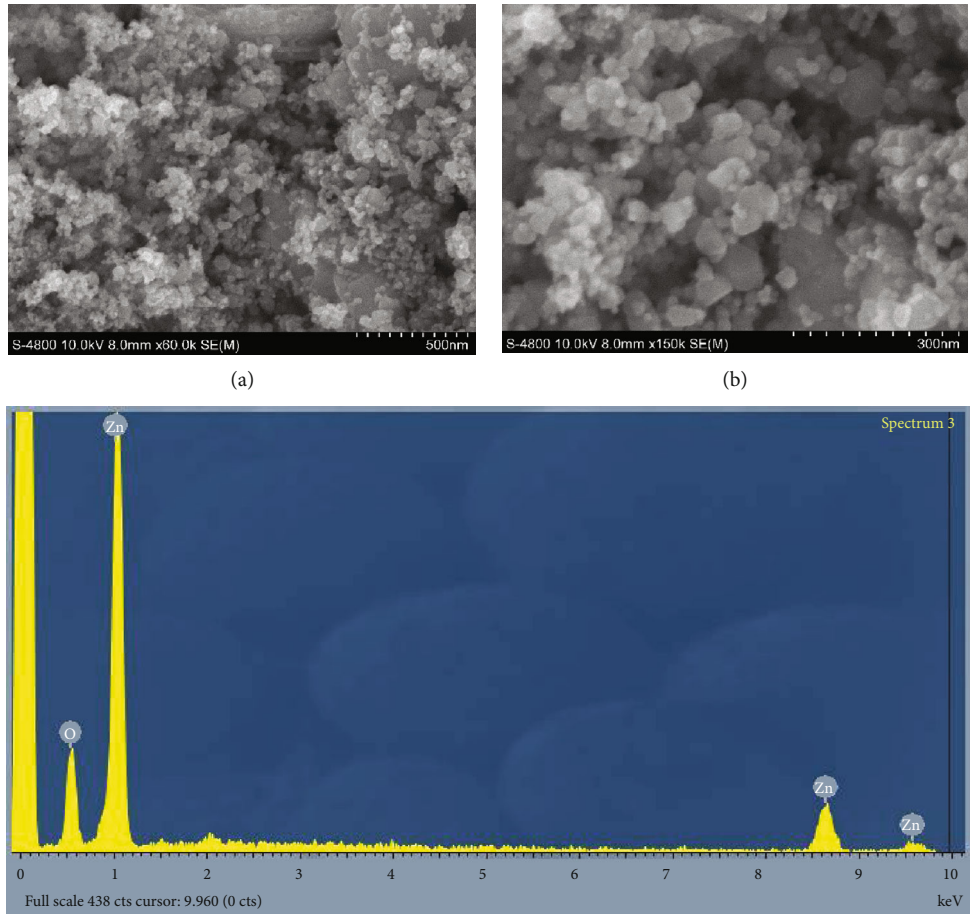

Figure 13: The morphology of ZnO NPs under SEM spectroscopy at a magnification of (a) 60 k và (b) 150 k; (c) EDX spectrum.

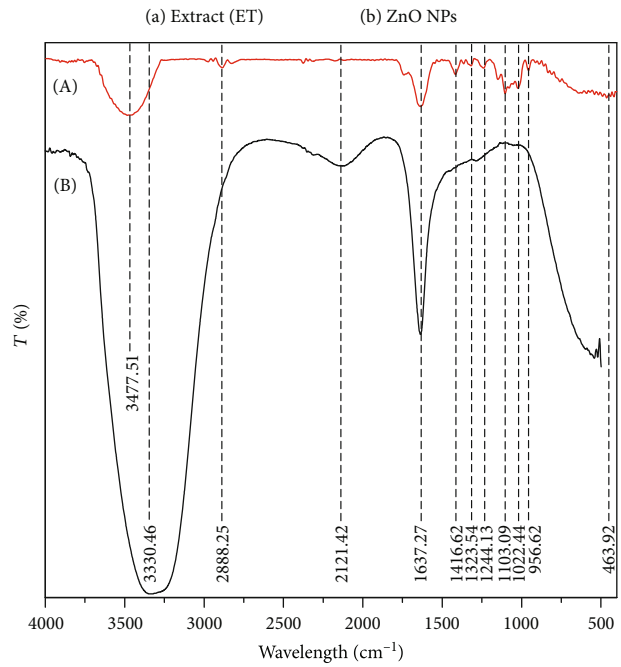

Figure 14: FT-IR spectra of (a) dry extract and (b) ZnO NPs.

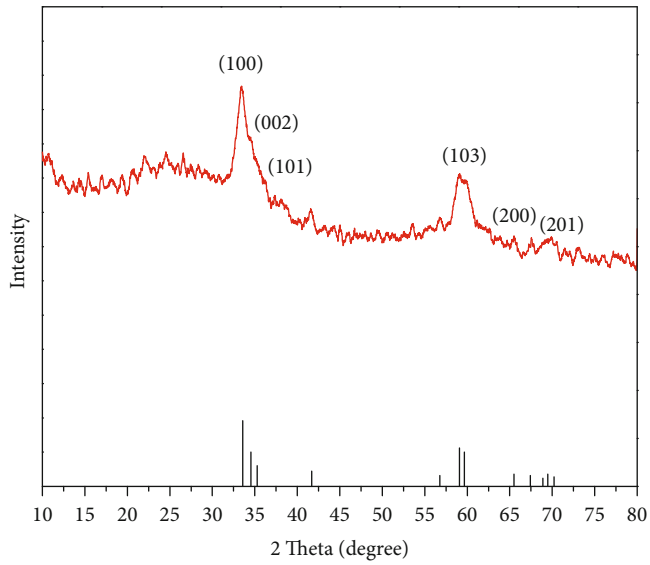

Figure 15: XRD pattern of ZnO NPs.

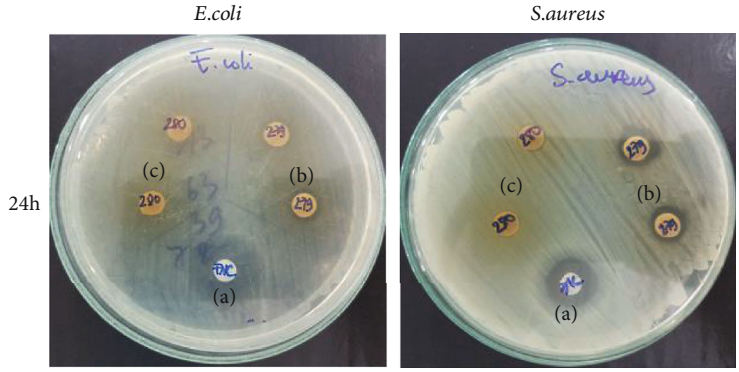

Figure 16: Antibacterial result of ET and ZnO NPs: (a) control, (b) ZnO NPs, and (c) extract.

Table 5: Zone of inhibition of ZnO NPs and ZnO NP-coated surgical sutures (hereinafter referred to as plus suture).

Bacteria	ZOI of ZnO NPs (mm)			
	24 h	48 h	72 h	120 h
E. coli	1	4	4	4
S. aureus	2	3	3	3

3.4.3. Bactericidal Test of ZnO NPs Coated on Surgical Sutures. Figure 18 exhibits that the ZnO-coated surgical suture has antibacterial ability compared with the control even after coating one time. This promising result proved that ZnO NPs are able to be applied in the medical device category.

4. Conclusions

In this study, a simple, low-cost method for the preparation of ZnO NPs using *Piper betle* leaf extract has been successfully achieved. There have been some evidences suggesting that green synthesis of ZnO NPs has enhanced the use in implantation. High-tech analysis has been used to demonstrate the formation of ZnO NPs. Apart from that, this study evaluated the size and morphology control based on the volume of *Piper betle* leaf extract. The ZnO NPs showed good antibacterial performance on *E. coli* and *S. aureus*, which are the main reasons for surgical site infection. The antibacterial effectiveness of ZnO NPs was observed up to 5 days, which is able to reduce the rate of SSI significantly. The results from bacteriological studies also confirmed that the antibacterial property of the ZnO NP-coated suture is better than that of the uncoated one, which is promising for applying ZnO NPs in the medical category.

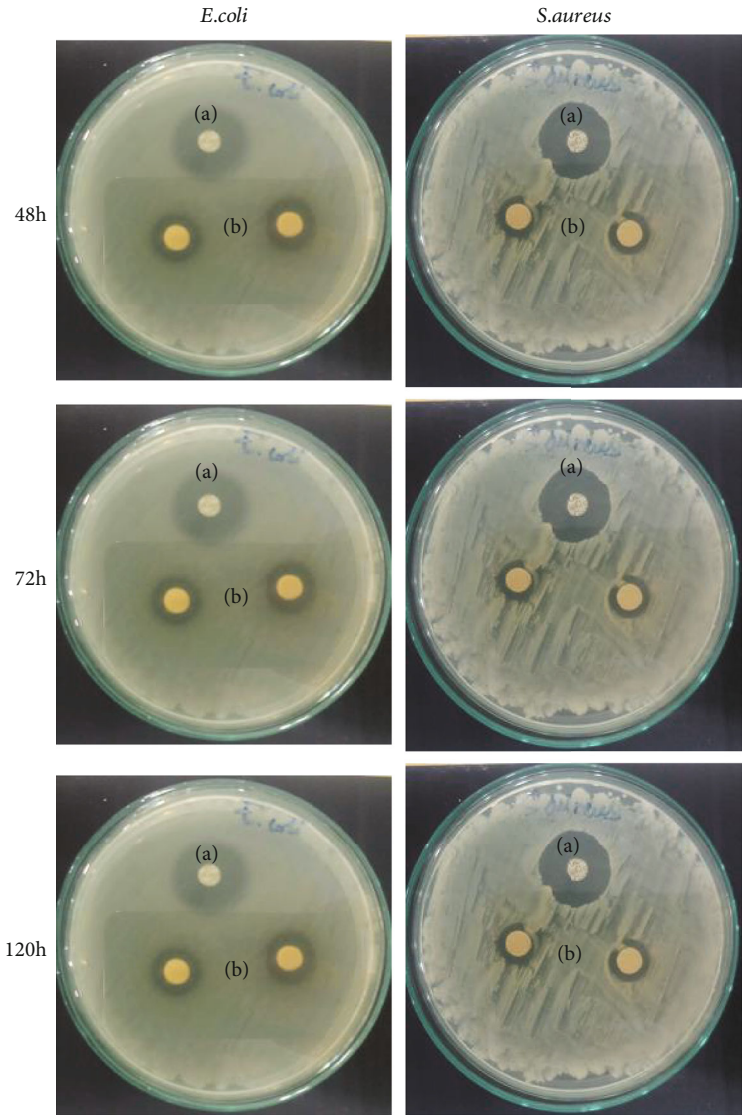

Figure 17: Zone of inhibition of ZnO NPs on *E. coli* and *S. aureus* at different times: (a) control and (b) ZnO NPs.

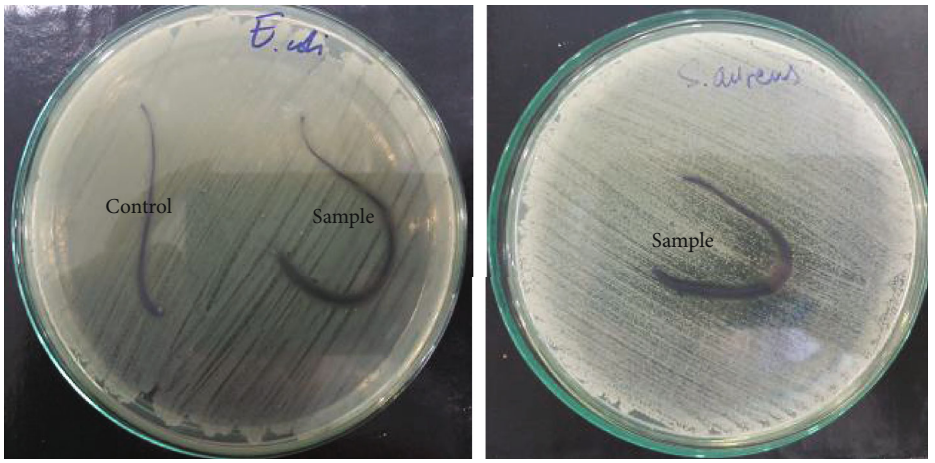

Figure 18: Zone of inhibition of control (ZnO-uncoated suture) and sample (ZnO-coated suture).

Data Availability

Raw data were generated at the faculty of chemical engineering, Industrial University of Ho Chi Minh City, Vietnam. Derived data supporting the findings of this study are available from the corresponding author on request.

Conflicts of Interest

The authors declare that there is no conflict of interest regarding the publication of this paper.

Authors' Contributions

Quynh Mai Thi Tran and Hong Anh Thi Nguyen contributed equally to the work.

Acknowledgments

This study is supported by the Industrial University of Ho Chi Minh City and Ho Chi Minh City University of Food Industry, Vietnam, for financial support.

References

[1] J. M. Badia, A. L. Casey, N. Petrosillo, P. M. Hudson, S. A. Mitchell, and C. Crosby, "Impact of surgical site infection on healthcare costs and patient outcomes: a systematic review in six European countries," *Journal of Hospital Infection*, vol. 96, no. 1, pp. 1–15, 2017.

[2] G. de Lissovoy, K. Fraeman, V. Hutchins, D. Murphy, D. Song, and B. B. Vaughn, "Surgical site infection: incidence and impact on hospital utilization and treatment costs," *American Journal of Infection Control*, vol. 37, no. 5, pp. 387–397, 2009.

[3] D. Gould, "Causes, prevention and management of surgical site infection," *Nursing Standard*, vol. 26, no. 47, pp. 47–56, 2012.

[4] C. D. Owens and K. Stoessel, "Surgical site infections: epidemiology, microbiology and prevention," *Journal of Hospital Infection*, vol. 70, Supplement 2, pp. 3–10, 2008.

[5] D. E. Fry, "Surgical site infection: pathogenesis and prevention," 2003, https://www.medscape.org/viewarticle/448981.

[6] A. M. Spagnolo, G. Ottria, D. Amicizia, F. Perdelli, and M. L. Cristina, "Operating theatre quality and prevention of surgical site infections," *Journal of Preventive Medicine and Hygiene*, vol. 54, no. 3, pp. 131–137, 2013.

[7] S. Morrison, A. Singh, J. Rousseau, and J. S. Weese, "Adherence of methicillin-resistantStaphylococcus pseudintermediusto suture materials commonly used in small animal surgery," *American Journal of Veterinary Research*, vol. 77, no. 2, pp. 194–198, 2016.

[8] K. R. Brown, C. P. Johnson, M. P. Goheen et al., "Bacterial adherence to surgical sutures: can antibacterial-coated sutures reduce the risk of microbial contamination?," *Journal of the American College of Surgeons*, vol. 203, no. 4, pp. 481–489, 2006.

[9] J. Dhom, D. A. Bloes, A. Peschel, and U. K. Hofmann, "Bacterial adhesion to suture material in a contaminated wound model: comparison of monofilament, braided, and barbed sutures," *Journal of Orthopaedic Research*, vol. 35, no. 4, pp. 925–933, 2017.

[10] J. R. Fowler, T. A. Perkins, B. A. Buttaro, and A. L. Truant, "Bacteria adhere less to barbed monofilament than braided sutures in a contaminated wound model," *Clinical Orthopaedics & Related Research*, vol. 471, no. 2, pp. 665–671, 2013.

[11] C. Mingmalairak, "Antimicrobial sutures: new strategy in surgical site infections," *Science against Microbial Pathogens: Communicating Current Research and Technological Advances: Formatex Research Center*, vol. 13, no. 23, pp. 313–323, 2011.

[12] A. Morad Asaad and S. Ahmad Badr, "Surgical site infections in developing countries: current burden and future challenges," *Clinical Microbiology: Open Access*, vol. 5, no. 6, 2016.

[13] M. Konop, T. Damps, A. Misicka, and L. Rudnicka, "Certain aspects of silver and silver nanoparticles in wound care: a minireview," *Journal of Nanomaterials*, vol. 2016, Article ID 7614753, 10 pages, 2016.

[14] L. Q. Chen, L. Fang, J. Ling, C. Z. Ding, B. Kang, and C. Z. Huang, "Nanotoxicity of silver nanoparticles to red blood cells: size dependent adsorption, uptake, and hemolytic activity," *Chemical Research in Toxicology*, vol. 28, no. 3, pp. 501–509, 2015.

[15] Z. Ferdous and A. Nemmar, "Health impact of silver nanoparticles: a review of the biodistribution and toxicity following various routes of exposure," *International Journal of Molecular Sciences*, vol. 21, no. 7, p. 2375, 2020.

[16] A. R. Gliga, S. Skoglund, I. O. Wallinder, B. Fadeel, and H. L. Karlsson, "Size-dependent cytotoxicity of silver nanoparticles in human lung cells: the role of cellular uptake, agglomeration and ag release," *Particle and Fibre Toxicology*, vol. 11, no. 1, p. 11, 2014.

[17] Y. Zhang, T. Nayak, H. Hong, and W. Cai, "Biomedical applications of zinc oxide nanomaterials," *Current Molecular Medicine*, vol. 13, no. 10, pp. 1633–1645, 2013.

[18] V. Parihar, M. Raja, and R. Paulose, "A brief review of structural, electrical and electrochemical properties of zinc oxide nanoparticles," *Reviews on Advanced Materials Science*, vol. 53, no. 2, pp. 119–130, 2018.

[19] Y. Gutha, J. L. Pathak, W. Zhang, Y. Zhang, and X. Jiao, "Antibacterial and wound healing properties of chitosan/poly(vinyl alcohol)/zinc oxide beads (CS/PVA/ZnO)," *International Journal of Biological Macromolecules*, vol. 103, pp. 234–241, 2017.

[20] E. Ozkan, E. Allan, and I. P. Parkin, "White-light-activated antibacterial surfaces generated by synergy between zinc oxide nanoparticles and crystal violet," *ACS Omega*, vol. 3, no. 3, pp. 3190–3199, 2018.

[21] R. Rajendra, C. Balakumar, H. A. M. Ahammed, S. Jayakumar, K. Vaideki, and E. Rajesh, "Use of zinc oxide nano particles for production of antimicrobial textiles," *International Journal of Engineering, Science and Technology*, vol. 2, no. 1, 2010.

[22] J. Jiang, J. Pi, and J. Cai, "The advancing of zinc oxide nanoparticles for biomedical applications," *Bioinorganic Chemistry and Applications*, vol. 2018, Article ID 1062562, 18 pages, 2018.

[23] A. A. Tayel, W. F. El-Tras, S. Moussa et al., "Antibacterial action of zinc oxide nanoparticles against foodborne pathogens," *Journal of Food Safety*, vol. 31, no. 2, pp. 211–218, 2011.

[24] A. A. Mostafa, "Antibacterial activity of zinc oxide nanoparticles against toxigenic Bacillus cereus and Staphylococcus aureus isolated from some Egyptian food," *International*

Journal of Microbiological Research, vol. 6, no. 2, pp. 145–154, 2015.

[25] L. Esteban-Tejeda, C. Prado, B. Cabal, J. Sanz, R. Torrecillas, and J. S. Moya, "Antibacterial and antifungal activity of ZnO containing glasses," *PLoS One*, vol. 10, no. 7, article e0132709, 2015.

[26] C. Rode, M. Zieger, R. Wyrwa et al., "Antibacterial zinc oxide nanoparticle coating of polyester fabrics," *Journal of Textile Science and Technology*, vol. 1, no. 2, pp. 65–74, 2015.

[27] A. S. Hameed, "A new coating for non-resorbable surgical suture," *Journal of University of Babylon for Pure and Applied Sciences*, vol. 26, no. 1, pp. 301–307, 2018.

[28] Y. Song and J. Yang, "Preparation and in-vitro cytotoxicity of zinc oxide nanoparticles against osteoarthritic chondrocytes," *Tropical Journal of Pharmaceutical Research*, vol. 15, no. 11, pp. 2321–2327, 2016.

[29] Y. Qian, J. Yao, M. Russel, K. Chen, and X. Wang, "Characterization of green synthesized nano-formulation (ZnO-A. *vera*) and their antibacterial activity against pathogens," *Environmental Toxicology and Pharmacology*, vol. 39, no. 2, pp. 736–746, 2015.

[30] K. Elumalai and S. Velmurugan, "Green synthesis, characterization and antimicrobial activities of zinc oxide nanoparticles from the leaf extract of *Azadirachta indica* (L.)," *Applied Surface Science*, vol. 345, pp. 329–336, 2015.

[31] K. Ali, S. Dwivedi, A. Azam et al., "Aloe vera extract functionalized zinc oxide nanoparticles as nanoantibiotics against multi-drug resistant clinical bacterial isolates," *Journal of Colloid and Interface Science*, vol. 427, pp. 145–156, 2016.

[32] V. G. Reshma and P. V. Mohanan, "Cellular interactions of zinc oxide nanoparticles with human embryonic kidney (HEK 293) cells," *Colloids and Surfaces B: Biointerfaces*, vol. 157, pp. 182–190, 2017.

[33] K. Schilling, B. Bradford, D. Castelli et al., "Human safety review of 'nano' titanium dioxide and zinc oxide," *Photochemical & Photobiological Sciences*, vol. 9, no. 4, pp. 495–509, 2010.

[34] W. Ji, D. Zhu, Y. Chen, J. Hu, and F. Li, "In-vitro cytotoxicity of biosynthesized zinc oxide nanoparticles towards cardiac cell lines of Catla catla," *Biomedical Research*, vol. 28, no. 5, 2017.

[35] M. Madhumita, P. Guha, and A. Nag, "Bio-actives of betel leaf (*Piper betle* L.): a comprehensive review on extraction, isolation, characterization, and biological activity," *Phytotherapy Research*, vol. 34, no. 10, pp. 2609–2627, 2020.

[36] A. Budiman, D. W. Rusnawan, and A. Yuliana, "Antibacterial activity of *Piper betle* L. extract in cream dosage forms against Staphylococcus aureus and propionibacterium acne," *Journal of Pharmaceutical Sciences and Research*, vol. 10, no. 3, pp. 493–496, 2018.

[37] T. Nalina and Z. Rahim, "The crude aqueous extract of *Piper betle* L. and its antibacterial effect towards Streptococcus mutans," *American Journal of Biotechnology and Biochemistry*, vol. 3, no. 1, pp. 10–15, 2007.

[38] R. Subashkumar, M. Sureshkumar, S. Babu, and T. Thayumanavan, "Antibacterial effect of crude aqueous extract of *Piper betle* L. against pathogenic bacteria," *International Journal of Research in Pharmaceutical and Biomedical Sciences*, vol. 4, no. 1, pp. 42–46, 2013.

[39] C. Sarma, P. Rasane, S. Kaur et al., "Antioxidant and antimicrobial potential of selected varieties of *Piper betle* L. (betel leaf)," *Anais da Academia Brasileira de Ciências*, vol. 90, no. 4, pp. 3871–3878, 2018.

[40] B. Patra, M. T. Das, and S. K. Dey, "A review on *Piper betle* L. nature's," *Journal of Medicinal Plants Studies*, vol. 4, no. 6, pp. 185–192, 2016.

[41] S. Saini, "*Piper betel* L.: a review of phytochemical and pharmacological profile," *International Education & Research Journal*, vol. 2, no. 2, pp. 81–83, 2016.

[42] U. Taukoorah, N. Lall, and F. Mahomoodally, "*Piper betle* L. (betel quid) shows bacteriostatic, additive, and synergistic antimicrobial action when combined with conventional antibiotics," *South African Journal of Botany*, vol. 105, pp. 133–140, 2016.

[43] M. A. Rahman, M. T. Hossain, and M. A. Hamid, "Antibacterial activity of polyaniline coated silver nanoparticles synthesized from Piper betle leaves extract," *Iranian Journal of Pharmaceutical Research*, vol. 15, no. 2, pp. 591–597, 2016.

[44] D. Ananda, S. T. Babu, C. G. Joshi, and M. Shantaram, "Synthesis of gold and silver nanoparticles from fermented and non fermented betel leaf," *Internasional Journal of Nanomaterials and Biostructures*, vol. 5, no. 1, pp. 20–23, 2015.

[45] P. S. Praba, J. Jeyasundari, and Y. B. A. Jacob, "Synthesis of silver nano particles using Piper betle and its antibacterial activity," *European Chemical Bulletin*, vol. 3, no. 10, pp. 1014–1016, 2014.

[46] S. P. Rao, K. Byrappa, N. Keerthiraj, J. Chatterjee, and M. S. Mustak, "Phyto-fabrication of ZnO nanoparticles using Piper betel aqueous extract and evaluation of its applicability in dentistry," *Pharmaceutical Nanotechnology*, vol. 6, no. 3, pp. 201–208, 2018.

[47] L. Muruganandam, A. Krishna, J. Reddy, and G. S. Nirmala, "Optimization studies on extraction of phytocomponents from betel leaves," *Resource-Efficient Technologies*, vol. 3, pp. 385–393, 2017.

[48] L. W. Foo, E. Salleh, and S. N. H. Mamat, "Extraction and qualitative analysis of Piper betle leaves for antimicrobial activities," *International Journal of Engineering Technology Science and Research*, vol. 2, pp. 1–8, 2015.

[49] T. C. Sumon Das, "A review on green synthesis of Ag NPs and ZnO NPs from diferent plants extract and their antibacterial activity against multi-drug resistant bacteria," *Journal of Innovatinos in Pharmaceutical and Biological Sciences*, vol. 5, no. 4, pp. 63–67, 2018.

[50] H. Agarwal, S. Venkat Kumar, and S. Rajeshkumar, "A review on green synthesis of zinc oxide nanoparticles - an eco-friendly approach," *Resource-Efficient Technologies*, vol. 3, no. 4, pp. 406–413, 2017.

[51] M. Anbuvannan, M. Ramesh, G. Viruthagiri, N. Shanmugam, and N. Kannadasan, "*Anisochilus carnosus* leaf extract mediated synthesis of zinc oxide nanoparticles for antibacterial and photocatalytic activities," *Materials Science in Semiconductor Processing*, vol. 39, pp. 621–628, 2015.

[52] S. Nagarajan and K. A. Kuppusamy, "Extracellular synthesis of zinc oxide nanoparticle using seaweeds of gulf of Mannar, India," *Journal of Nanobiotechnology*, vol. 11, no. 1, pp. 1–11, 2013.

[53] M. Alavi, N. Karimi, and I. Salimikia, "Phytosynthesis of zinc oxide nanoparticles and its antibacterial, antiquorum sensing, antimotility, and antioxidant capacities against multidrug resistant bacteria," *Journal of Industrial and Engineering Chemistry*, vol. 72, pp. 457–473, 2019.

[54] M. Alavi, N. Karimi, and T. Valadbeigi, "Antibacterial, antibiofilm, antiquorum sensing, antimotility, and antioxidant activities of green fabricated Ag, Cu, TiO2, ZnO, and Fe3O4NPs viaProtoparmeliopsis muralisLichen aqueous extract against multi-drug-resistant bacteria," *ACS Biomaterials Science and Engineering*, vol. 5, no. 9, pp. 4228–4243, 2019.

[55] M. Balouiri, M. Sadiki, and S. K. Ibnsouda, "Methods for _in vitro_ evaluating antimicrobial activity: a review," *Journal of Pharmaceutical Analysis*, vol. 6, no. 2, pp. 71–79, 2016.